CNWRA *A center of excellence in earth sciences and engineering*

A Division of Southwest Research Institute™
6220 Culebra Road • San Antonio, Texas, U.S.A. 78228-5166
(210) 522-5160 • Fax (210) 522-5155

May 9, 2001
Contract No. NRC–02–97–009
Account No. 20.01402.861

U.S. Nuclear Regulatory Commission
ATTN: Mrs. Deborah A. DeMarco
Two White Flint North
11545 Rockville Pike
Mail Stop T8A23
Washington, DC 20555

Subject: Programmatic Review of Poster

Dear Mrs. DeMarco:

The enclosed poster components are being submitted for programmatic review. These poster components will be assembled as a poster and will be presented at the American Geophysical Union Spring Meeting to be held May 29–June 2, 2001, in Boston, Massachusetts. The title of this poster is:

> "Numerical Modeling of Unsaturated Flow in Thick Vadose Zones of Fractured Rocks" by W. Illman and D. Hughson

Please note that this poster is based on an abstract previously submitted to NRC on March 8, 2001. Please advise me of the results of your programmatic review. Your cooperation in this matter is appreciated.

Sincerely,

Budhi Sagar
Technical Director

/ph
Enclosures
cc:

J. Linehan	K. Stablein	W. Patrick
B. Meehan	D. Brooks	CNWRA Directors
E. Whitt	B. Leslie	CNWRA Element Mgrs
J. Greeves	N. Coleman	T. Nagy (SwRI Contracts)
J. Holonich	H. Arlt	P. Maldonado
W. Reamer	L. Hamdan	W. Illman
T. Essig	J. Pohle	D. Hughson

Washington Office • Twinbrook Metro Plaza #210
12300 Twinbrook Parkway • Rockville, Maryland 20852-1606

Numerical Modeling of Unsaturated Flow in Thick Vadose Zones of Fractured Rocks

Walter A. Illman and Debra L. Hughson
Center for Nuclear Waste Regulatory Analyses, San Antonio, TX, 78238-5166, USA

ABSTRACT

Unsaturated flow through fractured rocks is a concern in the siting and performance of waste disposal facilities such as the proposed geological repository at Yucca Mountain, NV. Unsaturated flow in fractured rocks is uncertain primarily due to the highly heterogeneous properties of fractured media, interactions between the matrix and fractures, and the effect of boundary conditions such as episodic pulses of infiltration from storm events. We modeled flow in unsaturated fractured rocks using a two-phase, non-isothermal flow simulator. In this simulator the fractured rock is idealized as a dual-continuum porous medium, in which the matrix and fractures constitute distinct continua represented by two overlapping, interacting numerical grids. The exchange of fluids between the continua is governed by Darcy's law and the area of the matrix-fracture interface open to flow. To investigate the applicability of the dual-continuum approach for modeling unsaturated flow in a thick vadose zone of fractured rocks, we applied the model to site data collected from Yucca Mountain. A two-dimensional numerical model was constructed using uniform formation properties to investigate the effects of geologic layering on flow diversion. These model results showed agreement between modeled saturation and ambient saturation data obtained from deep boreholes at Yucca Mountain. However, heterogeneity of rock properties is a primary source of uncertainty in the spatial and temporal distribution of unsaturated flow through fractured rock. We investigated the consequences on unsaturated flow of simplifying fracture permeability continua by comparing the model results using uniform formation properties to a stochastic model that incorporates spatial variability of the fracture continua permeability within the layers as a random multivariate normal field. Monte Carlo simulations revealed the development of preferential pathways and flow focusing, both of which can have significant consequences on the performance of waste disposal facilities constructed in unsaturated, fractured rocks.

HIGHLIGHTS

- The primary objective of this study was to examine the effects of varying hydrogeologic strata properties on unsaturated flow through thick vadose zones. We modeled unsaturated flow numerically using site data collected at Yucca Mountain. The numerical model considered flow of water in three geologic units, each having distinct fracture and matrix properties based on the dual continuum concept. We compared those results to a model that treats spatial variability in the fracture permeability of each layer.

- We investigated the consequences on unsaturated flow of simplifying fracture permeability continua by comparing the model results using uniform formation

properties to modeling results from a stochastic model that incorporates spatial variability of the fracture continua permeability within the layers as a random multivariate normal field. Variability in fracture permeabilities can cause localized fast flow paths, perched waters, capillary barriers, and directional effects in fluid and gas flow.

- We conducted ten unconditional simulations to generate permeability fields with isotropic correlation scales for the Tiva Canyon unit. Ten additional realizations were generated to examine flow through the statistically anisotropic permeability field.

- We found that the variability in fracture permeability causes the development of preferential flow paths in the fracture continuum for the Tiva Canyon and Topopah Springs units and in the matrix continuum for the Paintbrush unit. Flow focusing due to the development of preferential pathways increases saturation locally. This local increase in saturation causes an increase in relative hydraulic conductivity along the pathway and reduces the exchange of water between the fracture and the matrix. The detection of these pathways may be difficult using traditional site characterization techniques.

STUDY OBJECTIVES

- To investigate the suitability of the dual continuum approach for modeling deep percolation in thick vadose zones of fractured rocks.
- To investigate the effect of layer stratification on water flow due to permeability and capillary barriers.
- To compare deterministic and stochastic continuum analyses of water flow in thick vadose zones of fractured rocks.
- To investigate the effect of geostatistical model structure (e.g., anisotropy in correlation scales) on flow and transport.
- To investigate the interaction between fractures and matrix on deep percolation.
- To investigate the effect of flow focussing on deep percolation in layered, heterogeneous media.
- To investigate the consequences of simplifying model structure and parameters on deep percolation.

MOTIVATION FOR THE STUDY

1. Spatially and temporally variable infiltration

- Modern climate scenario (CRWMS M&O, 2000)
  - Average precipitation rate: 188.5 mm/yr
  - Average outflow rate: 0.2 mm/yr
  - Mean infiltration rate: 3.6 mm/yr
  - Lower bound: 1.2 mm/yr
  - Upper bound: 8.8 mm/yr

(Include Figure 1 here.)

2. Geologic units of varying lithological and hydrogeological properties

- Tiva Canyon unit (TCw)
  - Moderately to densely welded tuff
  - Highly fractured near the soil surface
  - High fracture connectivity
  - Rapid transmittal of barometric pressure fluctuations
  - Flow primarily in fractures
  - Matrix porosity: 10%
  - Matrix saturation: 0.5 – 0.9

- Paintbrush unit (PTn)
  - Non-welded tuff
  - Low fracture density
  - Low fracture connectivity
  - Attenuation and lag in barometric signals through the unit
  - Smooth transitions in flow parameters near the contact between TCw/PTn
  - Abrupt transition in flow parameters near the contact between PTn/TSW
  - Flow thought to take place predominantly in the matrix
  - Matrix porosity – more than 30%
  - Matrix saturation: 0.4 – 0.7

- Topopah Springs member (TSw)
  - Welded, fractured tuff
  - Less fractured than TCw
  - High fracture connectivity
  - Rapid transmittal of barometric pressure fluctuations
  - Flow primarily in fractures
  - Matrix porosity - less than 9%
  - Matrix saturation: 0.5 – 0.9

(Include Plate 1 here.)

3. Elevated levels of Cl-36 in the ESF (Fabryka-Martin et al., 1996, 1997)

(Include Figure 2 here.)

COMPLEXITY OF UNSATURATED FLOW IN THICK VADOSE ZONES OF FRACTURED ROCKS

Estimation of percolation rates in thick vadose zones is complicated by:

- Episodic nature of precipitation events

- Localization of infiltration
- Poorly understood transport of water, air, and heat in the shallow subsurface
- Poorly understood constitutive relationships for unsaturated fractured rock.
- Spatial and temporal variability of water and air flow resulting from heterogeneity in rock properties at multiple scales
- Difficulty in measuring ambient percolation rates *in situ*

CONCEPTUALIZATION OF SITE HYDROGEOLOGY

DOE deterministic approach:

- Uniform, homogeneous parameters for each layer
- Parameters based on maximum likelihood
- Estimation using saturation, temperature, and pressure data
- Sensitivity analysis

(Include Figure 3 here.)

Proposed stochastic approach:

- Model individual layers
- Spatially vary fracture permeability for each layer
- Estimate statistics and geostatistical model structure from ongoing experiments
- Conduct Monte Carlo simulations

MASS AND ENERGY TRANSPORT (METRA) FEATURES

Numerical simulations were conducted using a two-phase, nonisothermal, dual continuum simulator METRA (Lichtner et al., 2000). METRA is based on a fully implicit formulation, and space discretization is based on a block-centered grid employing an integral finite-volume difference scheme suitable for an unstructured grid. The code uses various empirical relations to describe two-phase flow properties: most notably the van Genuchten (1980) function, which relates the relative permeability and saturation. The dual continuum technique was selected to model flow through the PTn unit. In this technique, the matrix and fracture constitute distinct continua and are represented by two (overlapping) grid blocks at each node. The exchange of fluids between the two continua is governed by Darcy's law and by the area of the matrix-fracture interface that is open to flow.

COMPUTATIONAL DOMAIN AND BOUNDARY CONDITIONS

Computational domain:

- 99 by 99 structured grid (9801 nodes)
- Overlapping gridblocks for fracture and matrix system (19602 nodes)
- 1 m blocks

- Rock properties:
  - Top 36 m: TCw
  - Next 33m: PTn
  - Last 30 m: TSw

Boundary conditions:

- Upper: Type 5 (Mixed/Cauchy) – specification of gas saturation, temperature, and liquid flux.
- Lower: Type 1 (Dirichlet) – constant field variables
- Side: Type 2 (Neumann) – no-flow boundary

MODEL RESULTS: HOMOGENEOUS CASE

The purpose of this effort was not to build a site model but to examine the effects of varying hydrogeologic strata properties on unsaturated flow through thick vadose zones. These results are compared to a model that incorporates spatial variability in the fracture permeability of each layer.

Model Parameters:

Parameters employed in this study were adapted from the unsaturated zone hydrology model developed for the Total System Performance Assessment-Viability Assessment (TSPA-VA) (CRWMS M&O, 1998). Tables 1a and b provide matrix and fracture parameter sets employed in the modeling study. The values listed are averaged values for the subunits of TCw, PTn, and TSw hydrogeologic units listed in the TSPA-VA. As our primary objective was not to reproduce flow through the subunits, the harmonic mean of the matrix and fracture permeability (k) of the subunits was used to calculate the permeability values for the composite TCw, PTn, and TSw units. The arithmetic mean of matrix and fracture porosities (ϕ), van Genuchten parameters (α, m, S_r), fracture frequency (f), and fracture-matrix connection area (X_{fm}) were used to obtain composite values. The subscripts m and f designate matrix and fracture, respectively.

Table 1a: Matrix parameter sets employed in this modeling study

Model layer	k_m [m^2]	ϕ_m	α_m [Pa^{-1}]	m_m	S_{rm}
TCw	9.68×10^{-18}	0.10	9.83×10^{-7}	0.33	0.23
PTn	1.29×10^{-14}	0.38	6.60×10^{-5}	0.33	0.12
TSw	8.32×10^{-17}	0.09	1.65×10^{-5}	0.26	0.08

Table 1b: Fracture parameter sets employed in this modeling study

Model layer	k_f [m^2] Vertical	k_f [m^2] Horizontal	ϕ_f	α_f [Pa^{-1}]	m_f	S_{rf}	f [m^{-1}]	X_{fm}
TCw	4.68×10^{-12}	4.62×10^{-13}	1.85×10^{-4}	1.93×10^{-4}	0.49	0.01	1.55	4.90×10^{-4}
PTn	1.25×10^{-13}	1.25×10^{-13}	6.69×10^{-5}	1.49×10^{-3}	0.45	0.01	0.55	3.10×10^{-1}
TSw	1.25×10^{-11}	8.29×10^{-13}	1.09×10^{-4}	6.66×10^{-5}	0.49	0.01	1.06	5.76×10^{-5}

The model run applied water uniformly at the top boundary at a rate of 8 mm/yr. Figures 4a and 4b show the steady state distribution of saturation in the fracture and matrix continua, respectively. Plotted alongside are contour plots of the flux magnitudes in the fracture (figure 4c) and matrix (figure 4d) continua.

Summary:

- To investigate the role of PTn properties on deep percolation, the model considered water flow in three geologic units, each having distinct fracture and matrix properties based on the dual continuum concept.

- In all three units, matrix permeability is significantly lower than fracture permeability, while the matrix porosity is significantly larger than fracture porosity. This contrast in flow properties between the fractures and matrix complicates the distribution of water as it flows through the strata. The interaction of fluid between the matrix and fracture necessitates the dual continuum approach.

- Water fluxes are highest in the fracture continuum in the TCw and TSw units and in the PTn matrix continuum.

- There is a buildup of saturation at the TCw/PTn contact in the fracture continuum, due to formation of a permeability barrier. As the saturation in the fracture continuum increases, it causes the imbibition of water into the PTn matrix. The water buildup in the matrix drains into the underlying PTn mostly as matrix flow.

- There is an increase in saturation at the PTn/TSw contact in the matrix continuum, due to formation of a capillary barrier. The buildup of saturation in the matrix continues until saturation is reached causing flow from the matrix into the fracture, allowing flow to continue down uniformly through the fracture continuum of the TSw unit.

(Include Figure 4 here.)

MODEL RESULTS: HETEROGENEOUS CASE

Heterogeneity of rock properties is a primary source of uncertainty in the spatial and temporal distribution of unsaturated flow through fractured rock. We investigated the consequences on unsaturated flow of simplifying fracture permeability continua by comparing the model results using uniform formation properties to those from a stochastic model that incorporates spatial variability of the fracture permeability continua within the layers as a random multivariate normal field. Variability in fracture permeabilities can cause localized fast flow paths, perched waters, capillary barriers, and directional effects in fluid and gas flow. No attempt was made to explicitly model discrete features including fractures, joints, and faults.

Model parameters:

Permeability fields were generated using a direct Fourier Transform Method developed by A. Gutjahr and his coworkers (Robin et al., 1996). Ten unconditional simulations were conducted to generate permeability fields with isotropic correlation scales for the TCw unit. Ten additional realizations were generated to examine flow through a statistically anisotropic permeability field.

Table 2 summarizes log-permeability statistics for the geostatistical simulation of a single layer model for the TCw unit. The purpose of this exercise was to investigate the role of geostatistical model structure (directionality in correlation lengths) on flow and transport. Available experimental data from the Yucca Mountain site are insufficient for determining the correlation structure of the fracture permeability field. Therefore, the log-permeability statistics in Table 2 are somewhat arbitrary, but are useful for evaluating model sensitivity to heterogeneity.

Table 2: Log-permeability statistics for geostatistical simulation of single layer model for the TCw unit.

Model	Mean	Variance	$\lambda_x\,[m]$	$\lambda_z\,[m]$
Exponential	-11.0	1.0	2.0	2.0
Exponential	-11.0	1.0	2.0	10.0

We modeled flow in the TCw unit to investigate the effect of heterogeneity in fracture permeability on water flux as it reaches the PTn unit. The model runs applied water uniformly at the top boundary at a rate of 4 mm/yr. Figures 5a through 5d show the steady state distribution of water flux in the fracture continuum with isotropic correlation lengths $\lambda_x = \lambda_z = 2$ m for realizations 1 through 4. Figures 6a through 6d show the corresponding realizations of fracture permeabilities used for the simulations.

Streamtraces are generated using the software TECPLOT v. 8. (Amtec Engineering, 1999) and are included to indicate flow paths in the fractures. A predictor-corrector integration scheme was employed to trace particles through a steady-state vector field generated by METRA. Figure 7 shows the steady state distribution of water flux in the fracture continuum from realization 1 at y = 90.5 m. The large variability in water flux is evident from this plot despite the uniform application of water at the top boundary. Figures 8a through 8d show the steady state distribution of water flux in the fracture continuum with anisotropic correlation lengths $\lambda_x = 2$ m and $\lambda_z = 10$ m for realizations 1 through 4. Figures 9a through 9d show the corresponding realizations of fracture permeabilities used for the simulations.

(Include Figure 5 here.)

(Include Figure 6 here.)

(Include Figure 7 here.)

(Include Figure 8 here.)

(Include Figure 9 here.)

We also generated a single realization of layered, heterogeneous media with varying statistical properties for each layer. Table 3 summarizes the log-permeability statistics for the geostatistical simulation for the 3-layer model. The model run applied water uniformly at the top boundary at a rate of 42.5 mm/yr. Figures 10a and 10b show the steady state distribution of saturation in the fracture and matrix continua, respectively. Plotted alongside are contour plots of the flux magnitudes in the fracture (figure 10c) and matrix (figure 10d) continua. Figures 11 shows the corresponding realization of fracture permeabilities used for the 3-layer simulation.

Table 3: Log-permeability statistics for geostatistical simulation of 3-layer model.

Model layer	Model	Mean [Log10]	Variance [Log10]	Correlation length [m]
TCw	Exponential	-11.8	1.0	2.0
PTn	Exponential	-12.9	1.0	2.0
TSw	Exponential	-11.5	1.0	2.0

Summary:

- Variability in fracture permeability causes the development of preferential flow paths in the fracture continuum for the TCw/TSw units and in the matrix continuum for the PTn unit. The development of preferential pathways in the fracture continuum increases the hydraulic conductivity along these pathways and reduces the exchange of water between the fracture and the matrix. The detection of these pathways may be difficult using traditional site characterization techniques.

- Preferential flow paths develop in the fracture and matrix despite the uniform application of water at the top boundary and without explicitly building in high permeability pathways or discrete features that represent fractures.

- Water flow rates in preferential flow pathways can be locally very high (more than ten times the input flow rate).

- Anisotropy in vertical correlation length causes the preferential pathways to be less tortuous (Figure 8a - d). Determination of geostatistical model structure through the spatial analysis of air permeability estimates obtained from single-hole pneumatic injection tests can be an important component in understanding deep percolation processes. Available experimental data from the Yucca Mountain site are insufficient for determining the geostatistical model and correlation structures of the fracture permeability field.

- The presence of the nonwelded PTn in the UZ led to the past conceptualization that deep percolation at Yucca Mountain becomes attenuated and laterally diverted once it

reaches the PTn unit. The 3-layer stochastic model (Figure 12 a - d) shows that (a) rapid flow takes place through persistent, preferential flow paths in the TCw and TSw units; (b) the focusing of flow at the TCw/PTn contact causes localized increases in matrix saturation that can extend from the TCw/PTn contact to the PTn/TSw contact, (c) increase in saturation causes the development of preferential pathways in the PTn matrix continuum; and (d) the preferential pathways allow for the rapid, predominantly downward movement of water through the unit.

- Comparison of results obtained from the homogeneous and heterogeneous model of unsaturated flow through thick vadose zones shows that deep percolation can take place rapidly through persistent, preferential flow paths. These pathways are hard to detect and may carry large volumes of water. Simplification of site hydrogeology may lead to erroneous conclusions on the spatial and temporal distribution of unsaturated flow through thick, fractured vadose zones. The consequences of simplifying model structure and parameters on deep percolation are currently under investigation.

Include Figure 10 here.

Include Figure 11 here.

REFERENCES

Amtec Engineering, 1999, *TECPLOT version 8.0 User's Manual*, Amtec Engineering, In., Bellevue, WA.

Civilian Radioactive Waste Management System Management and Operating Contractor, Chapter 2 *Total System Performance Assessment-Viability Assessment (TSPA-VA) Analyses Technical Basis Document, Unsaturated Zone Hydrology Model*, B00000000-01717-4301-00002 REV 00, Las Vegas, NV, Civilian Radioactive Waste Management System Management and Operating Contractor, 1998.

Civilian Radioactive Waste Management System Management and Operating Contractor, *Simulation of Net Infiltration for Modern and Potential Future Climates*, ANL-NBS-HN-000032, Rev. 00, Las Vegas, NV, Civilian Radioactive Waste Management System Management and Operating Contractor, 2000.

Fabryka-Martin, J. T., H. J. Turin, A. V. Wolfsberg, D. Brenner, P. R. Dixon, J. A. Musgrave, 1996, Summary Report of Chlorine-36 Studies. LA-CST-TIP-96-003, YMP Milestone Report 3782M, Los Alamos National Laboratory, Los Alamos, NM.

Fabryka-Martin, J. T., A. L. Flint, D. S. Sweetkind, A. V. Wolfsberg, S. S. Levy, G. J. C. Roemer, J. L. Roach, L. E. Wolfsberg, and M. C. Duff, 1997, Evaluation of flow and transport models of Yucca Mountain, based on chlorine-36 and chloride studies for FY97: Los Alamos National Laboratory, Yucca Mountain Project Milestone Report SP2224M3.

Flint, L. E., 1998, Characterization of hydrogeologic units using matrix properties, Yucca Mountain, Nevada, US Geological Survey Water Resources Investigation Report 98-4243, US Geological Survey, Denver, CO.

Lichtner, P. C., M. S. Seth, and S. Painter, 2000, MULTIFLO User's Manual, MULTIFLO Version 1.2, Two-phase Nonisothermal Coupled Thermal-Hydrologic-Chemical Flow Simulator, Center for Nuclear Waste Regulatory Analyses, San Antonio, Texas, Rev. 2 Change 0, January 2000.

Robin, M. J. L., A. L. Gutjahr, E. A. Sudicky, and J. L. Wilson, 1993, Cross-correlated random field generation with the direct Fourier Transform Method, Water Resources Research, Vol. 29, No. 7, 2385-2397.

van Genuchten, M. T., 1980, A closed-form equation for predicting the hydraulic conductivity of unsaturated soils, Soil Science Society America Journal, Vol. 44, No. 5, 892-898.

ACKNOWLEDGEMENTS

This poster was prepared to document work performed by the Center for Nuclear Waste Regulatory Analyses (CNWRA) for the U.S. Nuclear Regulatory Commission (NRC) under Contract No. NRC-02-97-009. The activities reported here were performed on behalf of the NRC Office of Nuclear Material Safety and Safeguards, Division of Waste Management.This work is an independent product of the CNWRA and does not necessarily reflect the views or regulatory position of the U.S. Nuclear Regulatory Commission.

The authors would like to thank Mr. James Winterle for his technical review, Mr. Pat Mackin for his programmatic review, P. Houston for her secretarial support, and Mr. Randall Fedors for the stimulating discussion on rock properties at Yucca Mountain.

LIST OF FIGURES

Figure 1: Estimated net infiltration (mm/yr) for the mean modern climate scenario (adapted from CRWMS M&O, 2000).

Figure 2: Ratio of 36-Cl as sampled at regular intervals and at specific features along the Exploratory Studies Facility. Elevated ratios interpreted as bomb-pulse are indicated with diamond symbols.

Figure 3: East-west vertical cross-section along SD-7 showing stratigraphy and faults used in the development of the 3-D, site-scale, UZ-flow model (adapted from (CRWMS M&O, 1998).

Figure 4: Steady state distribution of: a) fracture saturation; b) matrix saturation; c) fracture water flux; and d) matrix water flux.

LIST OF PLATES

LIST OF TABLES

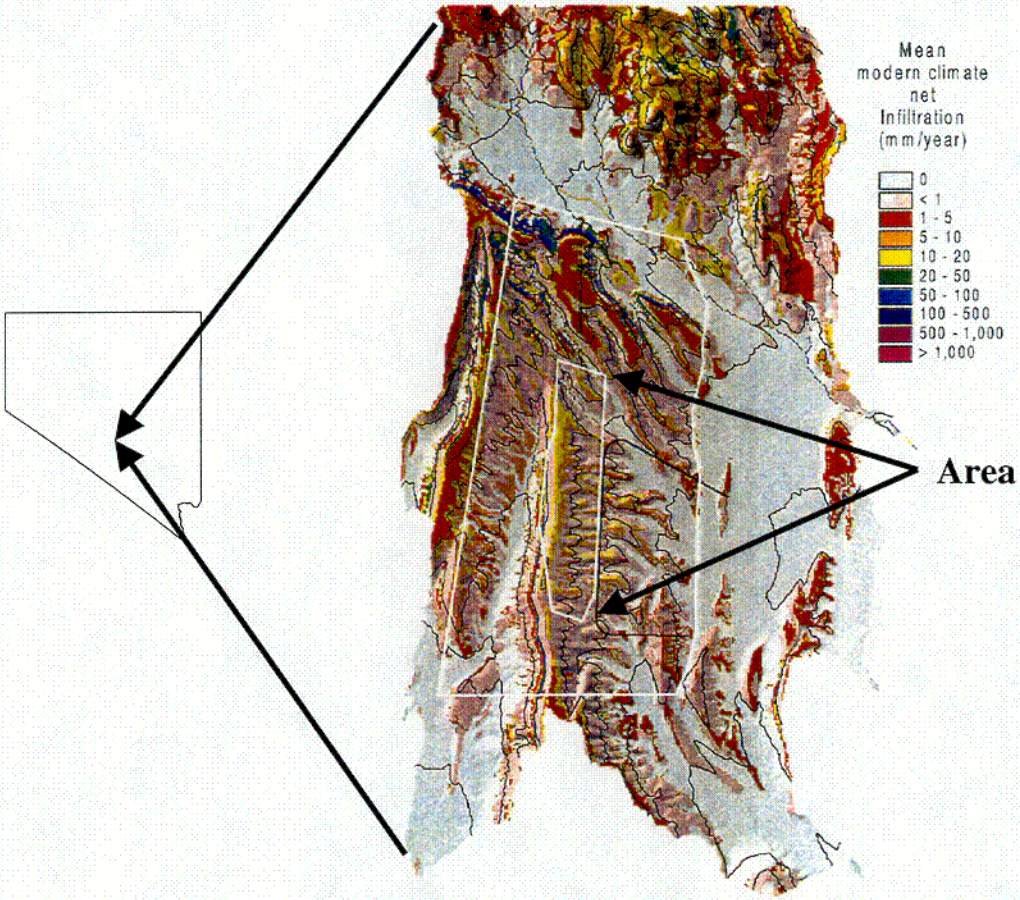
Mean
modern climate
net
Infiltration
(mm/year)
0
< 1
1 - 5
5 - 10
10 - 20
20 - 50
50 - 100
100 - 500
500 - 1,000
> 1,000
Area of proposed repository

C01

Fig. 1

Refined stratigraphy

TCw 12

TCw 13

PTn 21

PTn 22

PTn 23

PTn 24

PTn 25

TSw 31

TSw 32

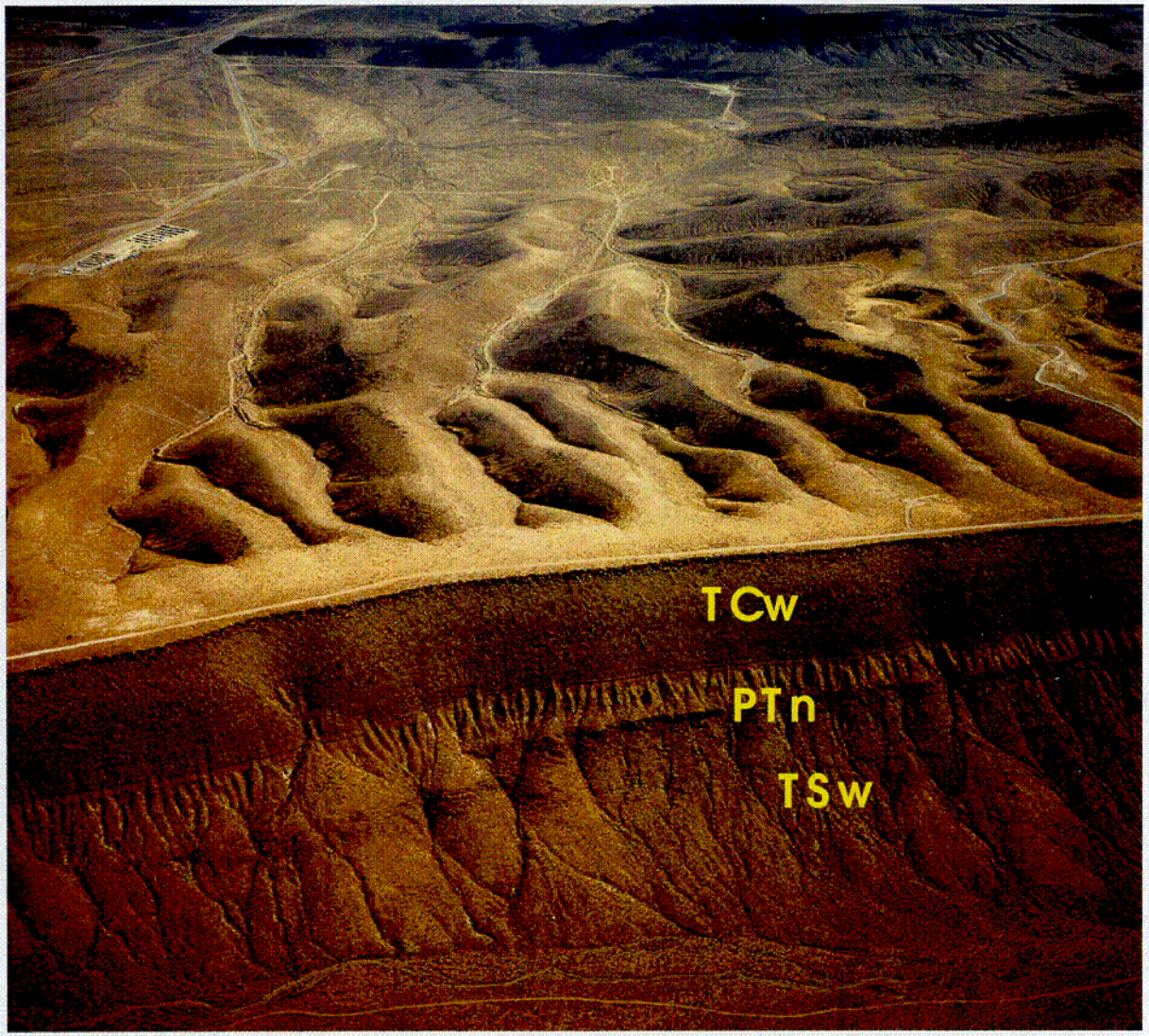

Stratigraphy for this modeling study

TCw

PTn

TSw

C02 Plate 1

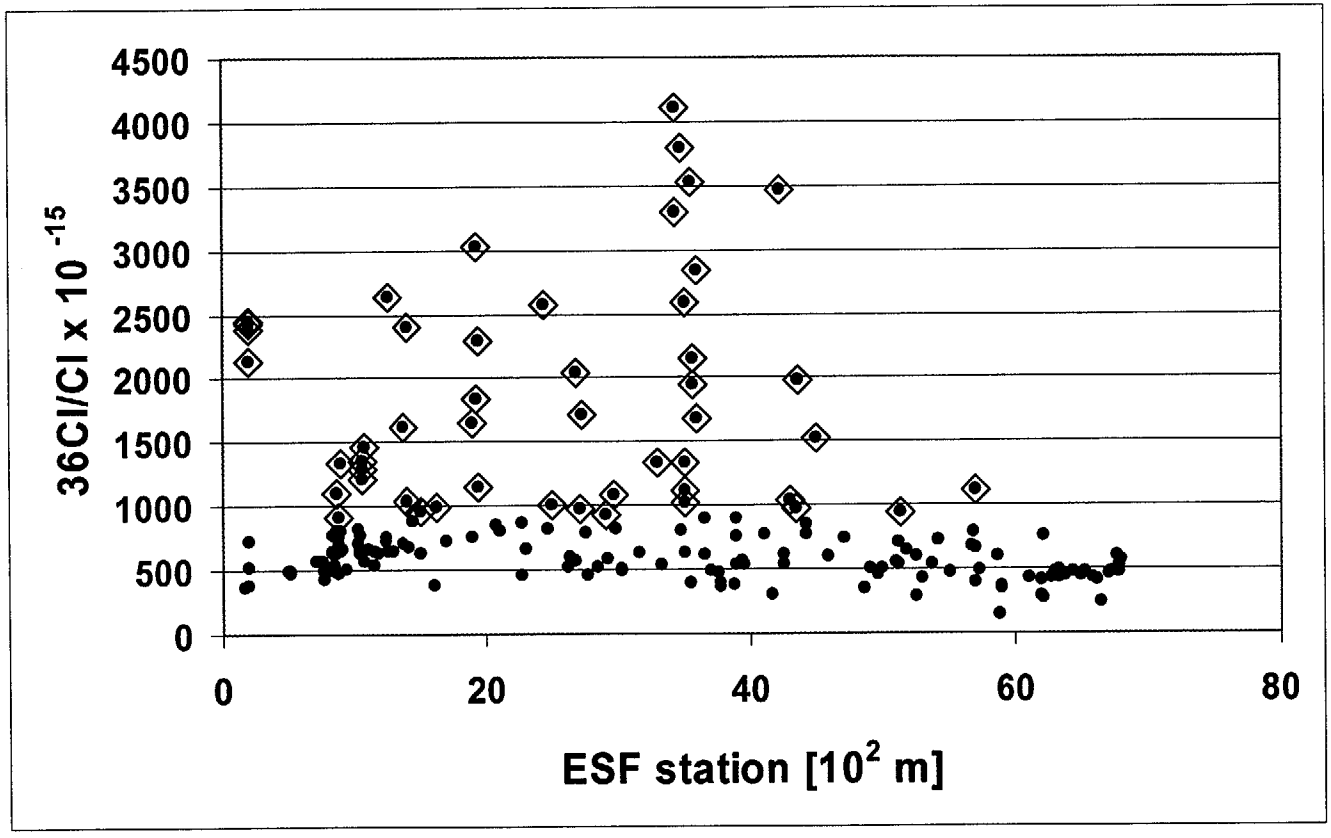
4500
4000
3500
3000
2500
2000
1500
1000
500
0
36Cl/Cl x 10 -15
0
20
40
60
80
ESF station [10^2 m]

Fig. 2

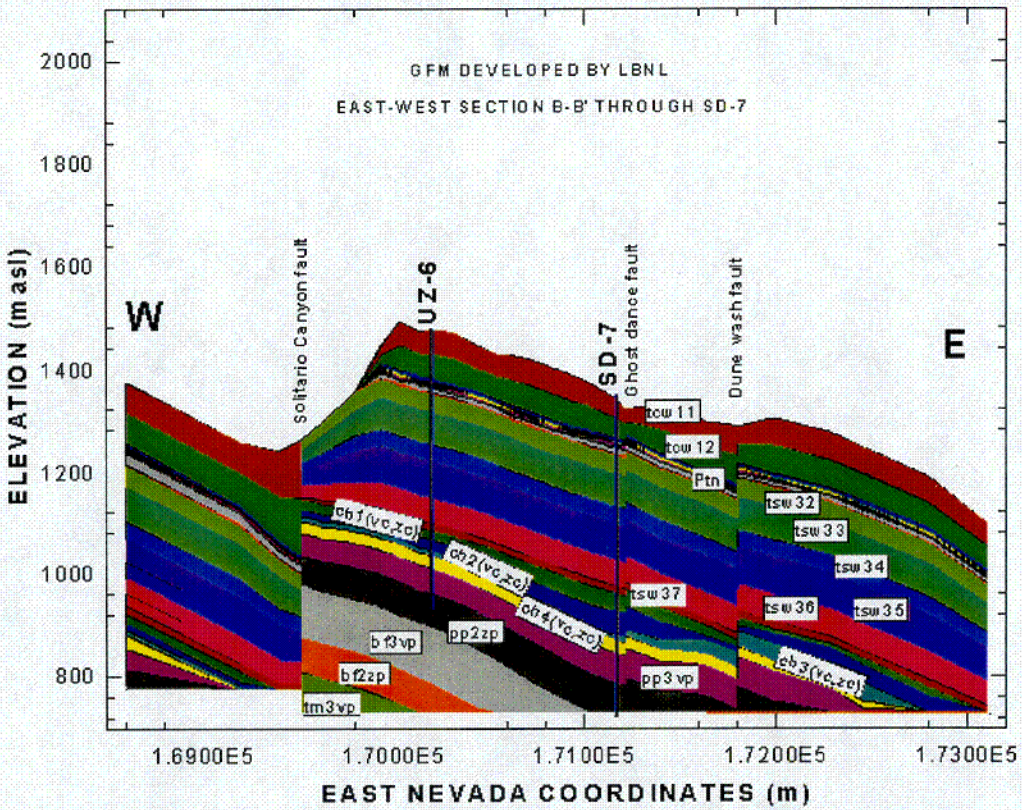
GFM DEVELOPED BY LBNL
EAST-WEST SECTION B-B' THROUGH SD-7
W
E
UZ-6
SD-7
Solitario Canyon fault
Ghost dance fault
Dune wash fault
ELEVATION (masl)
2000
1800
1600
1400
1200
1000
800
tcw 11
tcw 12
Ptn
tsw 32
tsw 33
tsw 34
tsw 35
tsw 36
tsw 37
ch1(vc,zc)
ch2(vc,zc)
ch3(vc,zc)
ch4(vc,zc)
pp2zp
pp3vp
bf3vp
bf2zp
tm3vp
1.6900E5
1.7000E5
1.7100E5
1.7200E5
1.7300E5
EAST NEVADA COORDINATES (m)

Fig. 3

a)

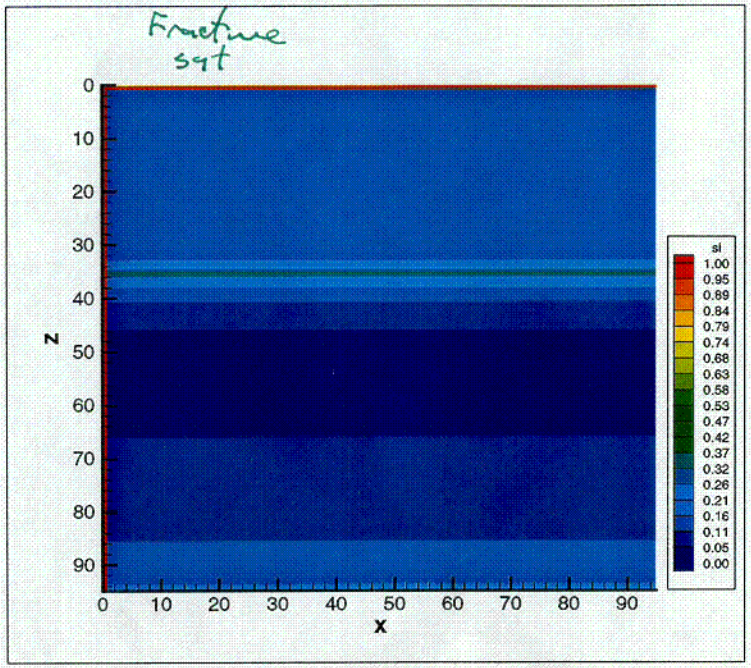

c)

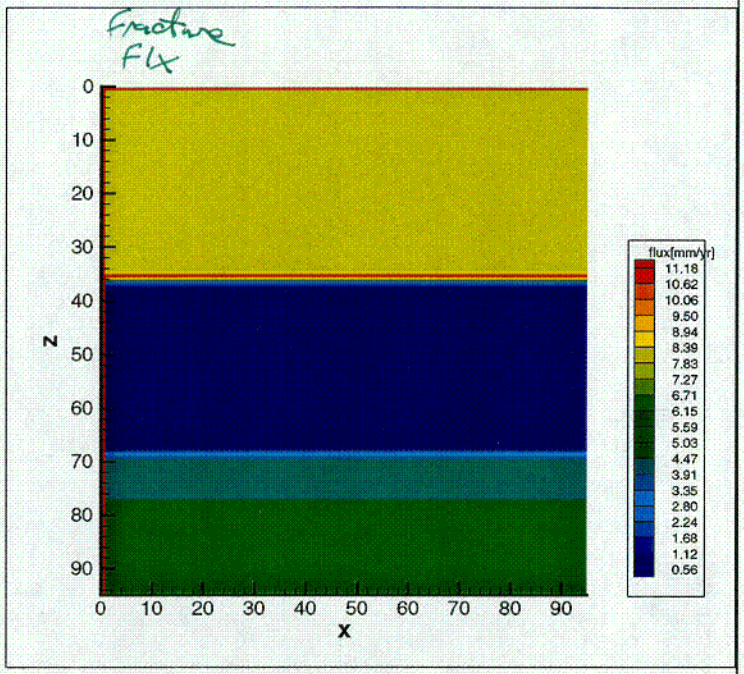

b)

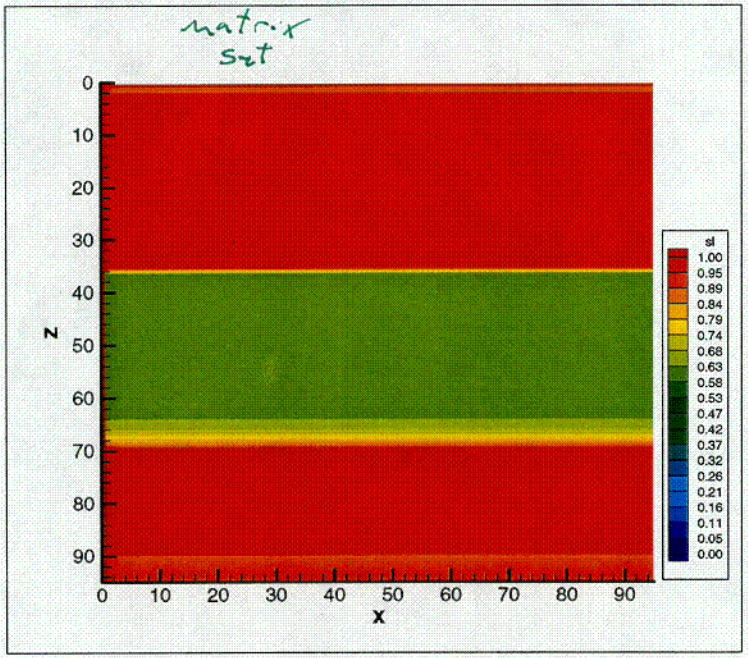

d)

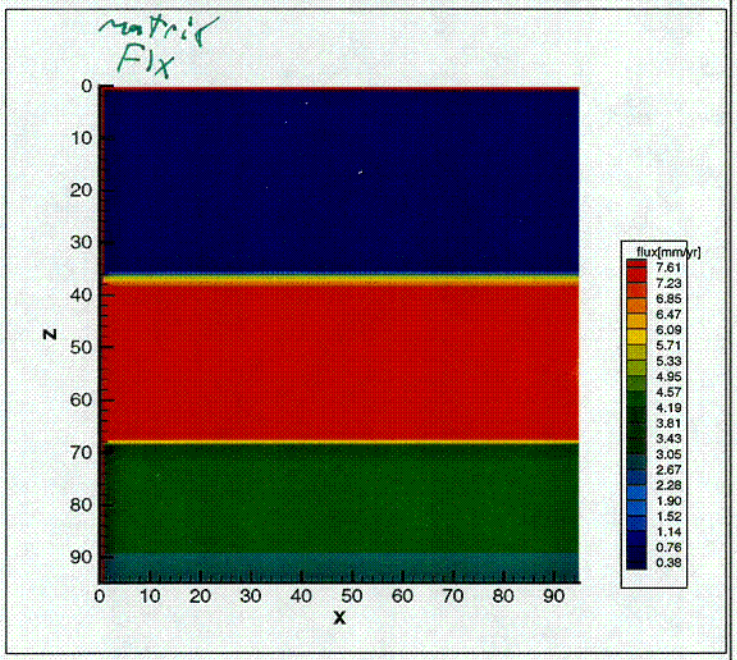

Fig 4a-d.

C04

a)

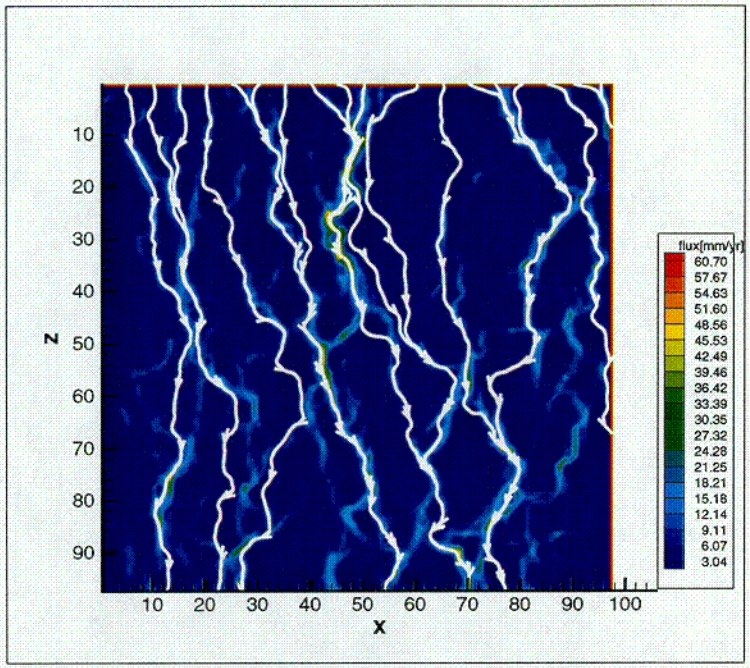

c)

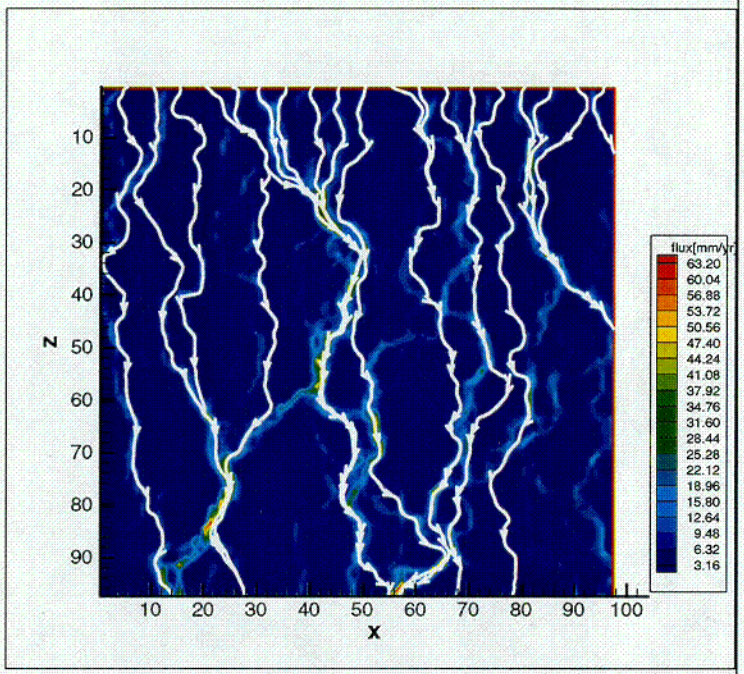

b)

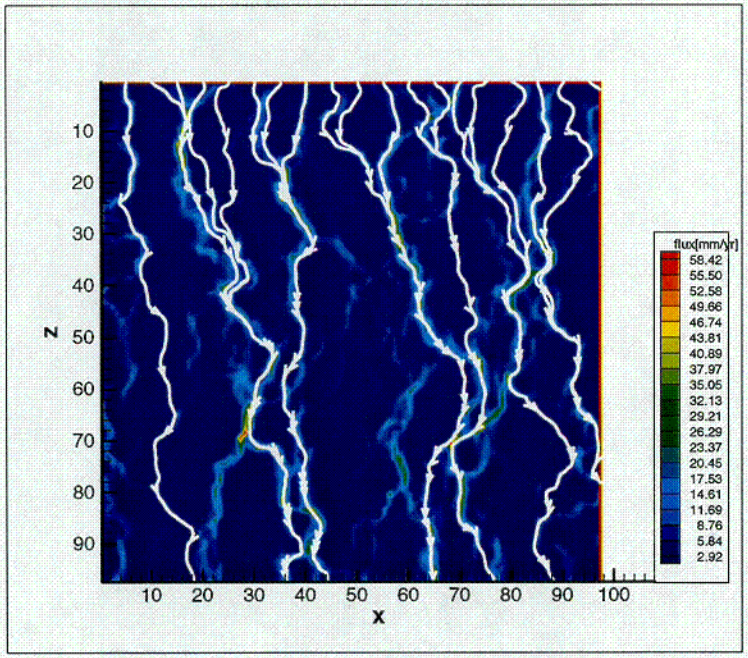

d)

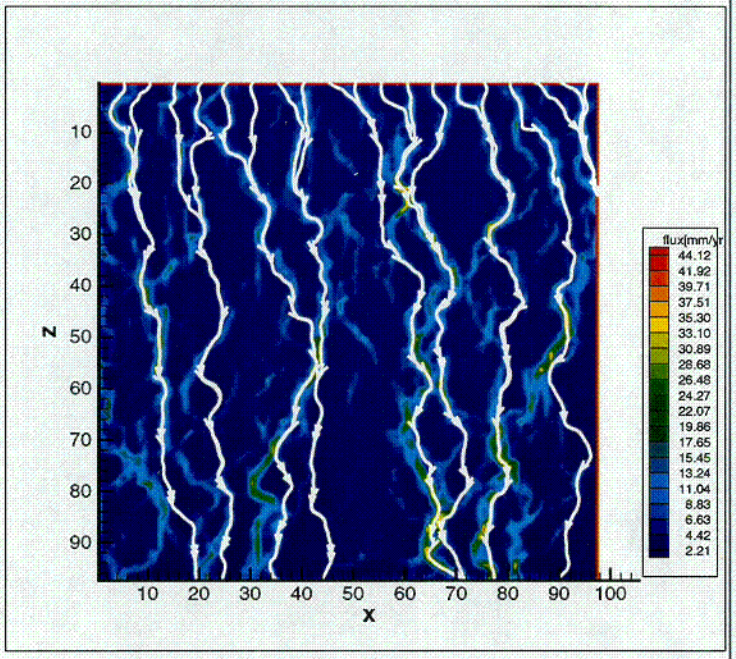

C05

Fig. 5a – 5d

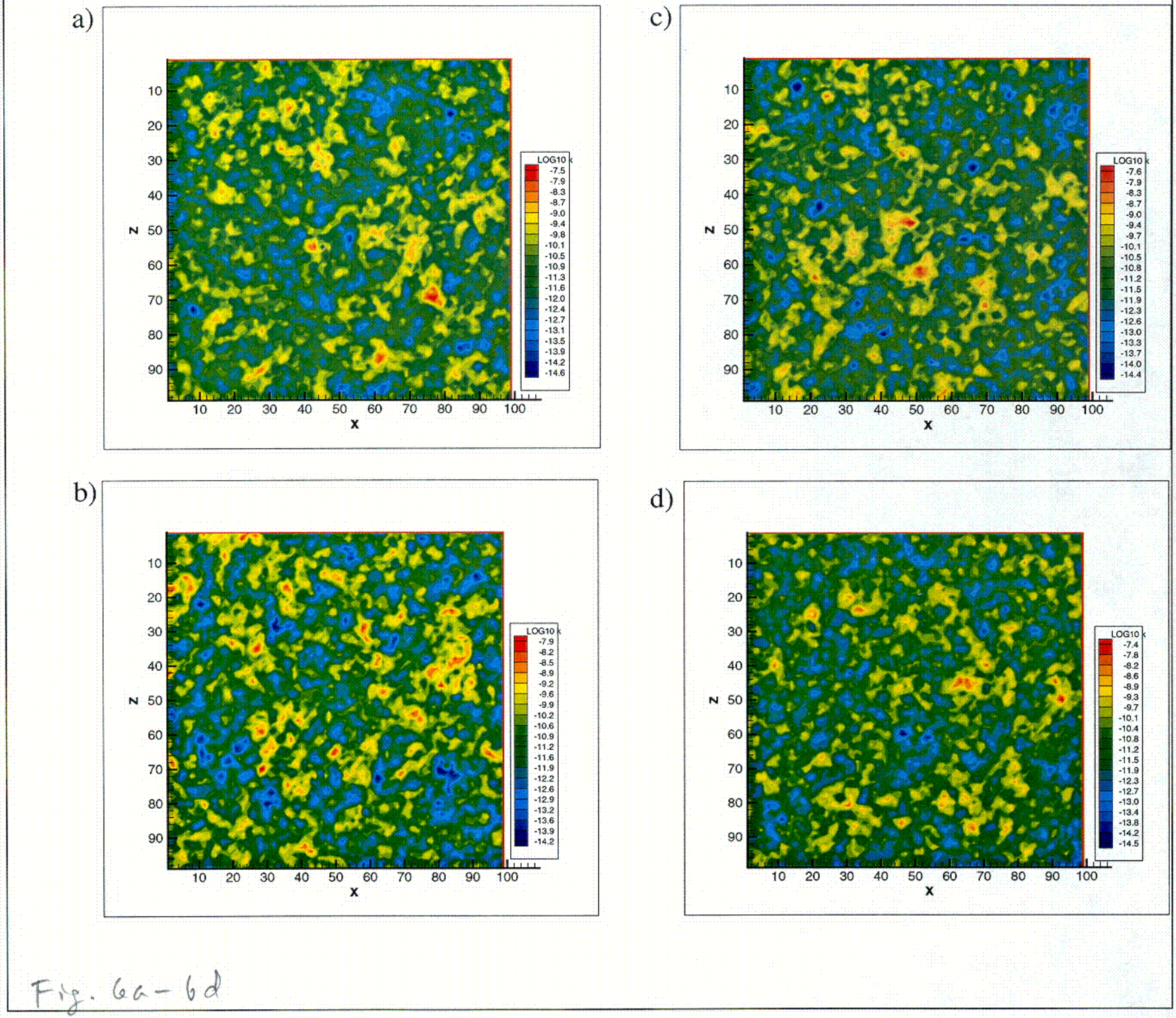

Fig. 6a – 6d

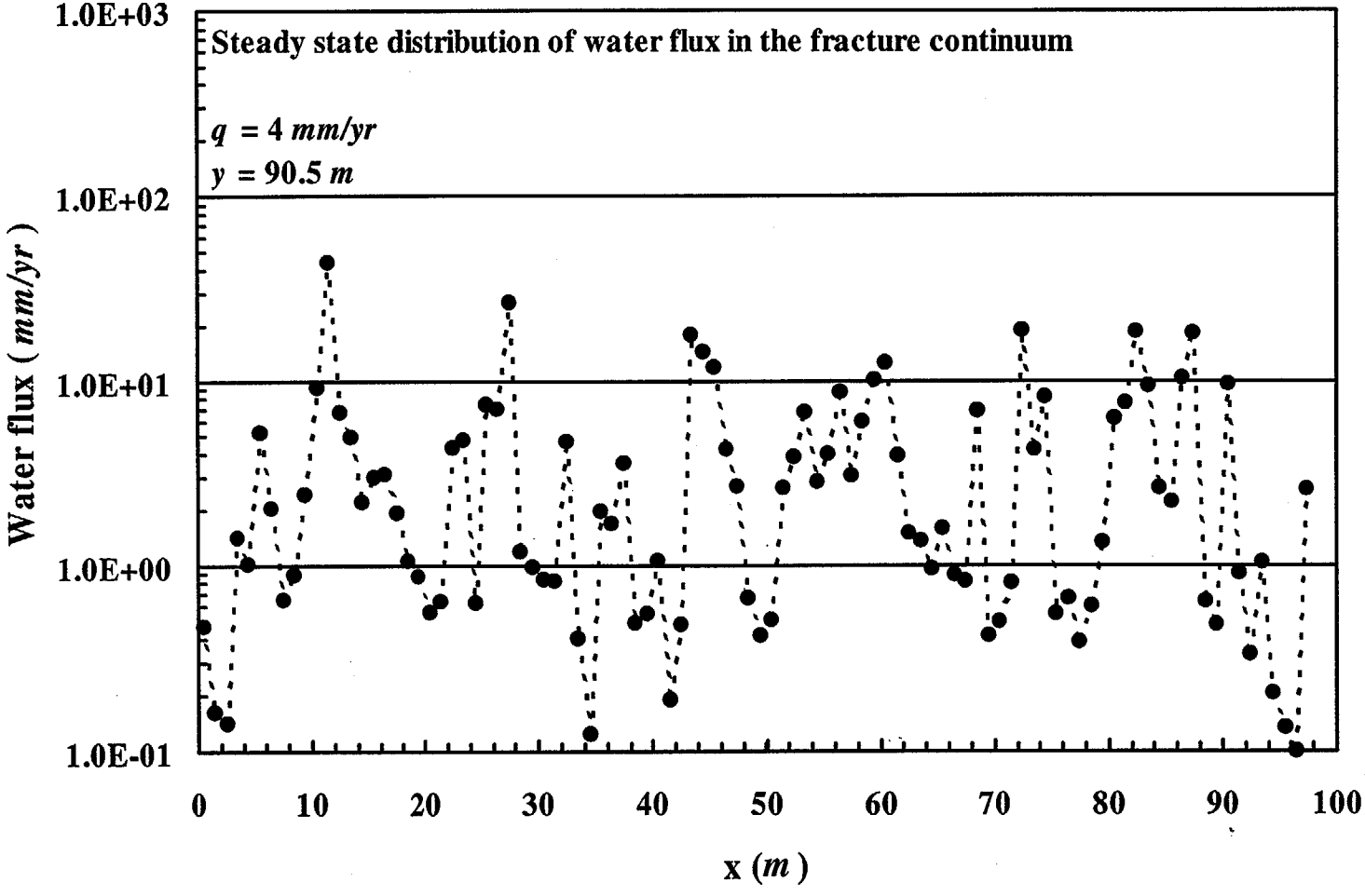
Steady state distribution of water flux in the fracture continuum
q = 4 mm/yr
y = 90.5 m
1.0E+03
1.0E+02
1.0E+01
1.0E+00
1.0E-01
Water flux (mm/yr)
0
10
20
30
40
50
60
70
80
90
100
x (m)

F-8 7

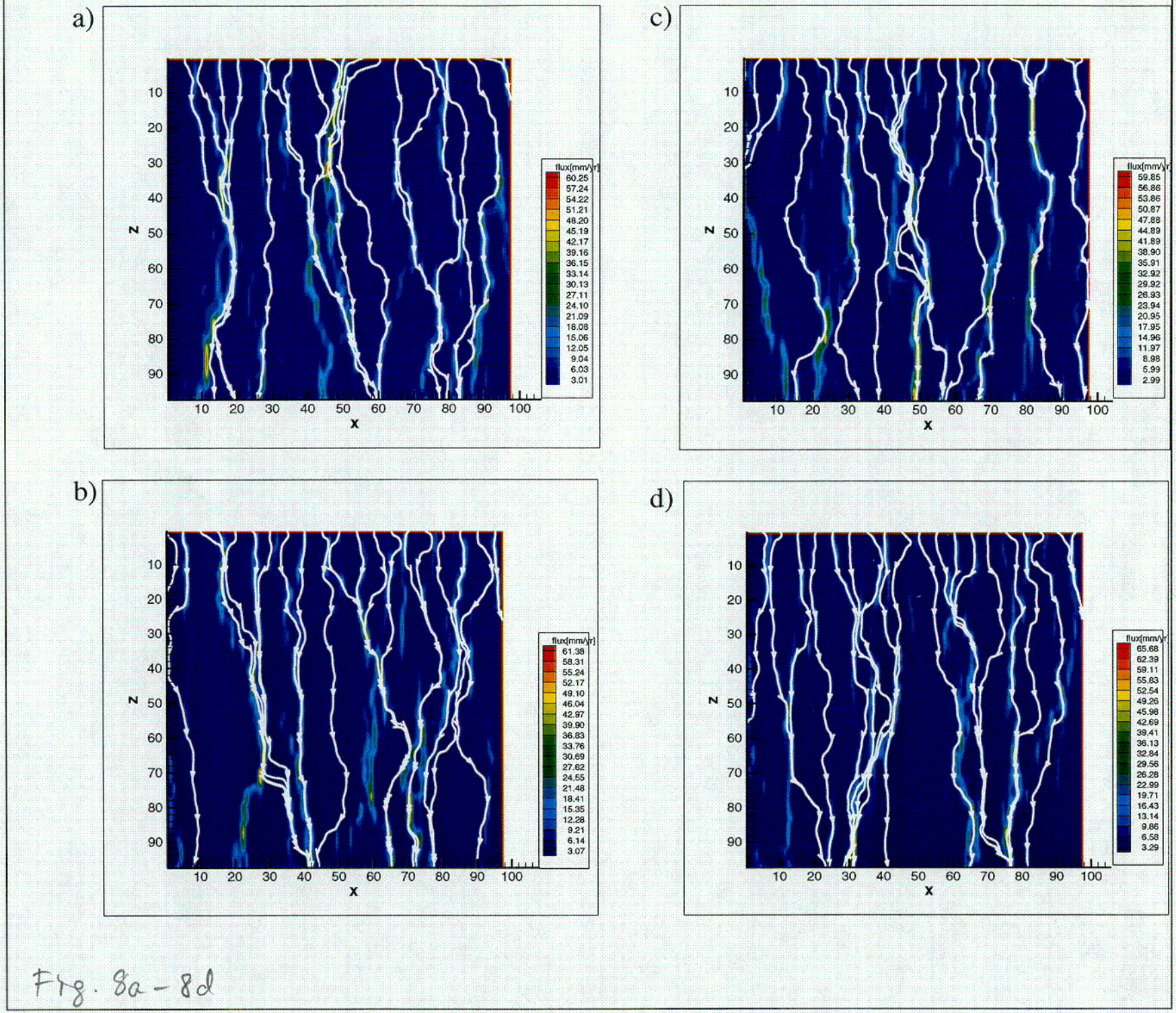
a)
b)
c)
d)
z
x
flux[mm/yr]
60.25
57.24
54.22
51.21
48.20
45.19
42.17
39.16
36.15
33.14
30.13
27.11
24.10
21.09
18.08
15.06
12.05
9.04
6.03
3.01
61.38
58.31
55.24
52.17
49.10
46.04
42.97
39.90
36.83
33.76
30.69
27.62
24.55
21.48
18.41
15.35
12.28
9.21
6.14
3.07
59.85
56.86
53.86
50.87
47.88
44.89
41.89
38.90
35.91
32.92
29.92
26.93
23.94
20.95
17.95
14.96
11.97
8.98
5.99
2.99
65.68
62.39
59.11
55.83
52.54
49.26
45.98
42.69
39.41
36.13
32.84
29.56
26.28
22.99
19.71
16.43
13.14
9.86
6.58
3.29

Fig. 8a – 8d

L07

a)

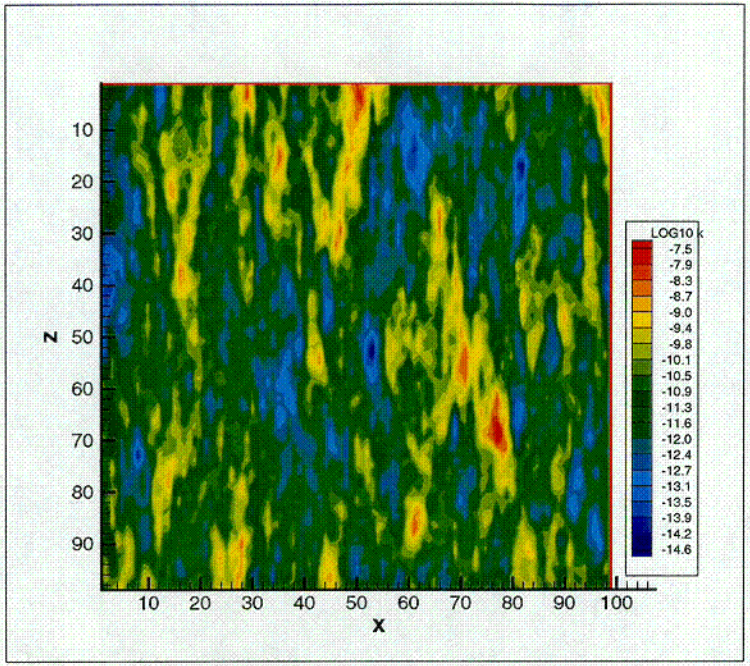

c)

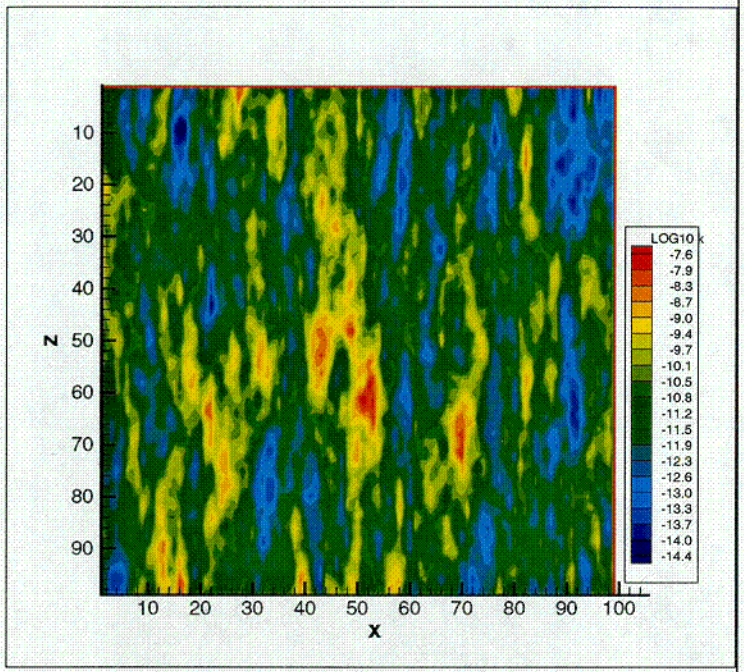

b)

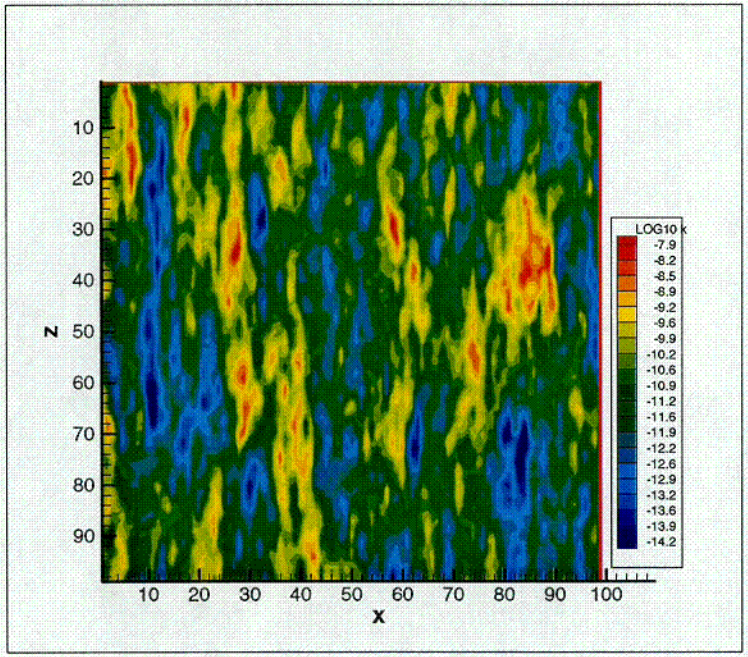

d)

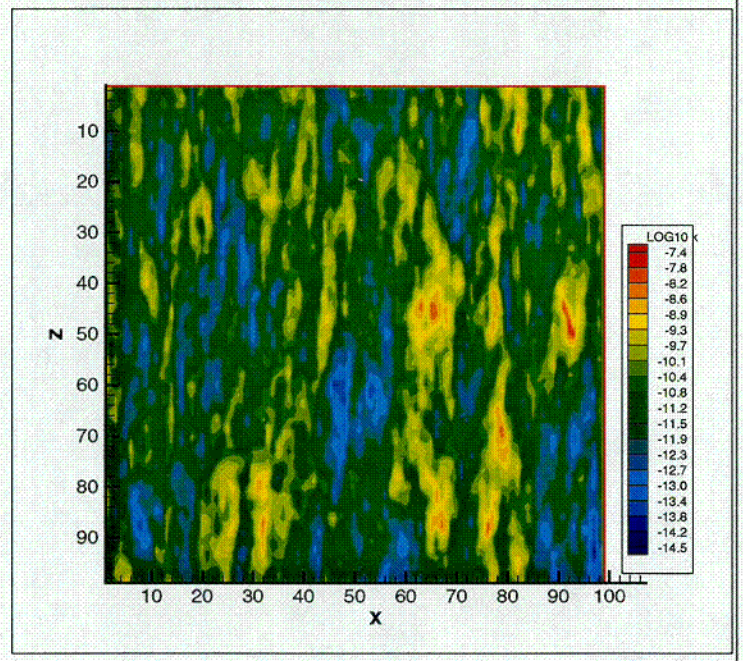

Fig 9a - 9d

C08

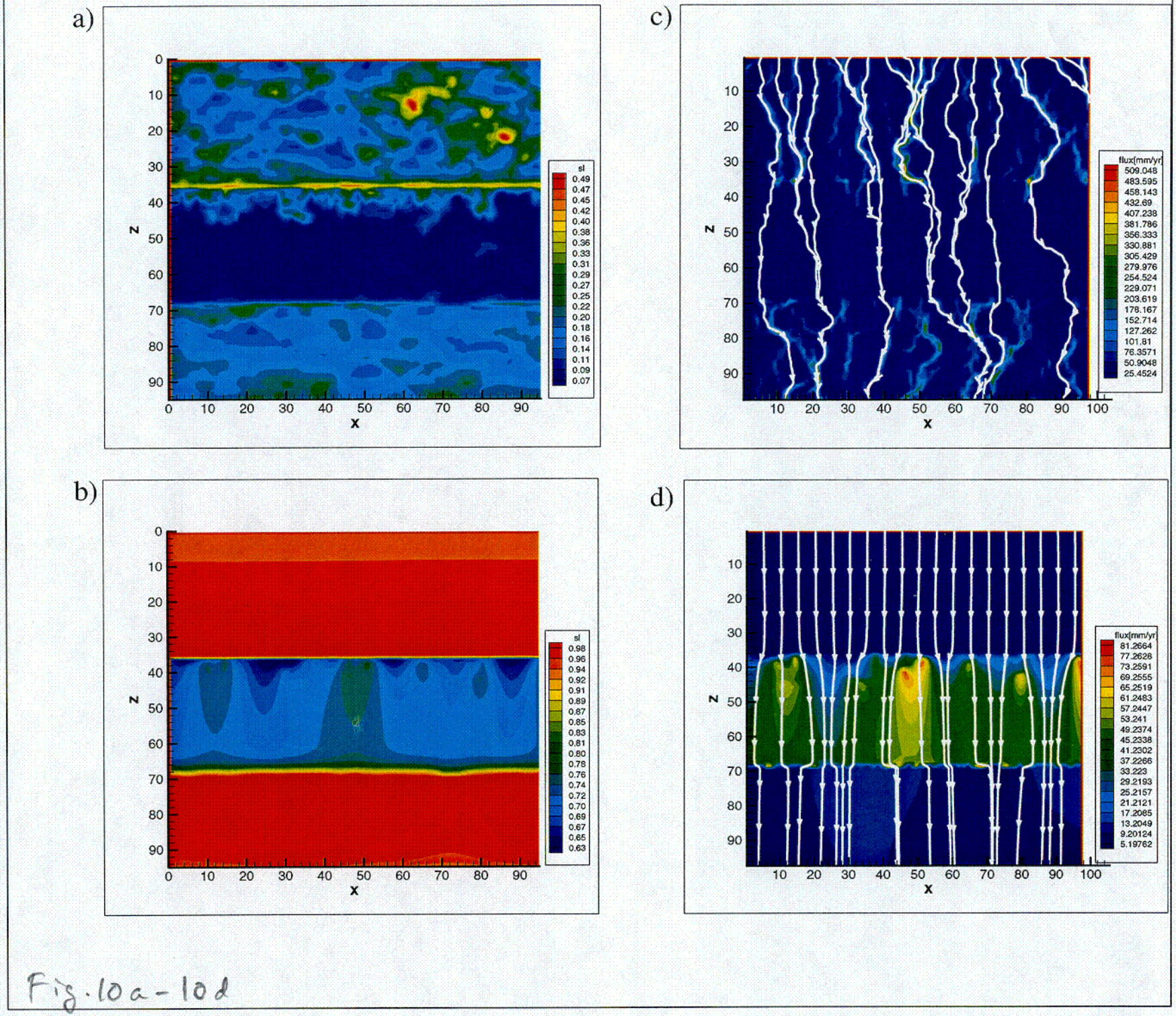

Fig. 10a - 10d

C09

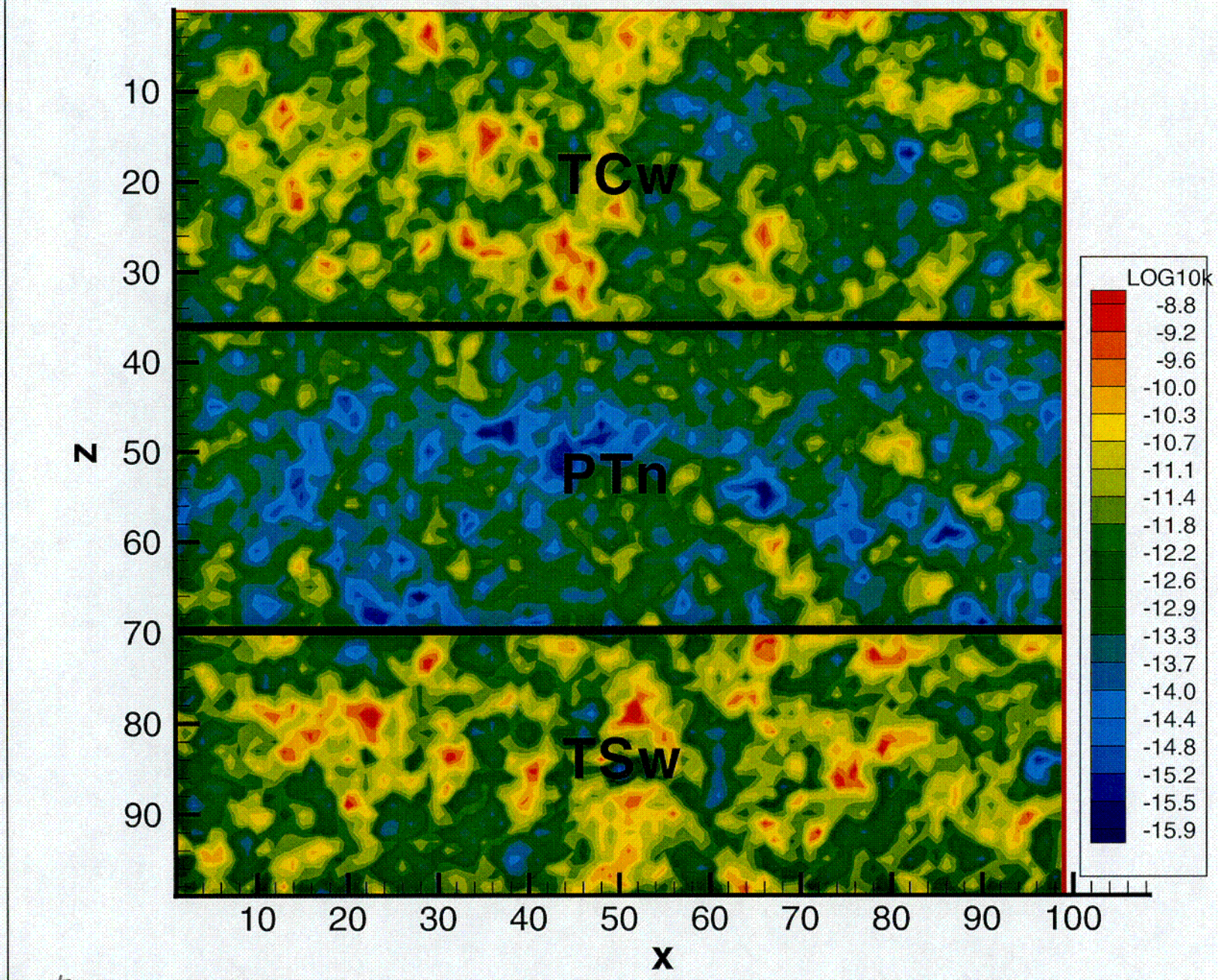
TCw
PTn
TSw
N
X
10
20
30
40
50
60
70
80
90
100
LOG10k
-8.8
-9.2
-9.6
-10.0
-10.3
-10.7
-11.1
-11.4
-11.8
-12.2
-12.6
-12.9
-13.3
-13.7
-14.0
-14.4
-14.8
-15.2
-15.5
-15.9

Fig. 11